Applied Energy 152 (2015) 156–161

Contents lists available at ScienceDirect

Applied Energy

journal homepage: www.elsevier.com/locate/apenergy

Investigation on the thermoacoustic conversion characteristic of regenerator

Zhanghua Wu [a], Yanyan Chen [a], Wei Dai [a], Ercang Luo [a,*], Donghui Li [a,b]

[a] Key Laboratory of Cryogenics, Chinese Academy of Sciences, Beijing 100190, China
[b] University of Chinese Academy of Sciences, Beijing 100049, China

HIGHLIGHTS

- A novel experimental setup was developed to investigate the regenerator performance.
- This approach was proved to control the phase angle of the engine efficiently.
- A highest thermal efficiency of 35.6% was achieved with random fiber regenerator.
- Flow resistance and heat transfer area are crucial to design a regenerator.

ARTICLE INFO

Article history:
Received 4 December 2013
Received in revised form 7 October 2014
Accepted 9 February 2015
Available online 12 March 2015

Keywords:
Regenerator
Thermoacoustic conversion
Linear motor

ABSTRACT

Regenerator is the core component in the regenerative heat engines, such as thermoacoustic heat engine, and Stirling heat engine. The regenerator has a porous configuration, in which the thermoacoustic effect happens between the working gas and solid wall converting heat into acoustic work. In this paper, a novel experimental setup was developed to investigate the thermoacoustic conversion characteristic of the regenerator. In this system, two linear motors acted as compressors to provide acoustic work for the regenerator and the other two linear motors served as alternators to consume the acoustic work out of the regenerator. By changing the impedance of the alternators, the phase difference between the volume velocities at the two ends of the regenerator could be varied within a large range. In the experiments, the influence of phase difference, heating temperature and different materials on the performance of the regenerator were studied in detail. According to the experimental results, the output acoustic power increased when the phase difference between velocities of the compression and expansion pistons increased within this phase angle range. And the thermoacoustic efficiency had different optimum values with different heating temperatures. Additionally, it also shows that flow resistance and heat transfer area were very important to the performance. In the experiments, a maximum output acoustic power of 715 W and a highest thermoacoustic efficiency of 35.6% were obtained with stack and random fiber type regenerators respectively under 4 MPa pressurized helium and 650 °C heating temperature. This work provides an efficient way to investigate the thermoacoustic conversion characteristic of the regenerator. It also provides some clues to the regenerator design.

1. Introduction

Regenerative heat engines, such as thermoacoustic engines and Stirling engines, are capable of converting external heat to mechanical work with high efficiency. This mechanical work can be further used to produce electricity or realize heat pumping from low temperature to high temperature. Thereby, these engines are quite suitable for solar energy and industrial waste heat application areas. Nowadays, more and more researchers are paying their attentions on these machines.

Regenerator is the core component in the regenerative heat engines, in which high-frequency oscillating flow gas converts heat absorbing from the solid to acoustic work. This phenomenon is called the thermoacoustic effect [1]. Due to a porous structure, the flow and heat exchanging conditions in the regenerators are very complicate. Thermoacoustic theories were founded by Rott [2–4], Swift [5], Backhaus [6] and Xiao [7–9] to reveal the thermoacoustic conversion characteristic of the regenerator and other components. It showed that the thermoacoustic conversion

* Corresponding author. Tel./fax: +86 10 82543750.
E-mail address: ecluo@mail.ipc.ac.cn (E. Luo).

http://dx.doi.org/10.1016/j.apenergy.2015.02.054
0306-2619/

Nomenclature

Symbols

A	area (m^2)
A_h	heat transfer area (m^2)
c_p	isobaric heat capacity per unit mass (J/kg/K)
D	diameter (m)
d_{wire}	wire diameter (m)
d_{gap}	flow channel gap of the stack (m)
i	imaginary unit
K	spring constant (N/m)
k	thermal conductivity (W/m/K)
L	electrical inductance (H)
l	length (m)
m	moving mass (kg)
P_0	mean pressure (Pa)
p	pressure amplitude (Pa)
Q	heating power
R_m	mechanical damping factor (kg/s)
R	load resistance (Ω)
r	resistance of the alternator winding (Ω)
T	temperature (K)
U	volume velocity (m^3/s)
V	volume (m^3)
V_b	volume of back space (m^3)
W	acoustic power (W)
x	displacement (m)
β	thermal expansion coefficient (K^{-1})
γ	specific heat ratio
η	thermoacoustic efficiency
θ	phase angle (°)
ρ	density, (kg/m^3)
τ	transduction coefficient (N/A)
Φ	porosity of regenerator
ω	angular frequency (rad/s)

characteristic of the regenerator is mainly determined by the acoustic field, temperature gradient, structure, and so on. The acoustic field means the phase difference between the pressure and the velocity waves. Experimental and numerical works also have been performed to describe the regenerator. In 2002, Ueda et al. studied the acoustic field of the regenerator in a loop configuration engine [10]. In 2004, Biwa et al. investigated the thermoacoustic conversion performance of the regenerator driven by a loudspeaker [11]. They adjusted the position of the regenerator in the experiments trying to obtain different acoustic fields of the regenerator. In 2013, Lawn investigated the acoustic pressure losses in the regenerator [12] and Kato et al. studied the regenerator efficiency of Stirling engine [13]. However, in these experiments, the obtained acoustic fields were very limited and the experiment processes were inconvenient. In recent years, Computational Fluid Dynamics (CFD) technology has been applied to investigate the regenerative systems, including engines [14–16] and cryocoolers [17,18]. However, the numerical results also need further verification by experiments. In this paper, in order to deeply and conveniently investigate the thermoacoustic conversion characteristic of the regenerator with different acoustic field conditions, a novel experimental setup was developed and the performance of the regenerator was evaluated.

In the following sections, the experimental setup is presented first as well as the typical structural parameters. Secondly, the experimental principle is introduced. Then, the experimental investigation is presented in detail. Lastly, some conclusions are made.

2. Experimental apparatus

Fig. 1 shows the schematic and photograph of the experimental apparatus developed in this paper. As demonstrated in Fig. 1(a), the setup consists of a linear compressor, a linear alternator and a thermoacoustic engine sandwiched between them. The engine includes a compression space, a main ambient heat exchanger, a regenerator, a hot-end heat exchanger, a thermal buffer tube, a secondary ambient heat exchanger and an expansion space. The hot-end heat exchanger and main ambient heat exchanger provide a temperature gradient along the regenerator, which is required by the thermoacoustic conversion effect. The thermal buffer tube is used to avoid the alternator piston working within a high temperature environment. The compressor is used to provide acoustic work for the regenerator, the acoustic work will be amplified by the regenerator under the temperature gradient. The alternator converts the acoustic work outputted by the regenerator into electricity, which will be consumed by a load resistance connected with the alternator. The working principle of the system will be introduced in next section.

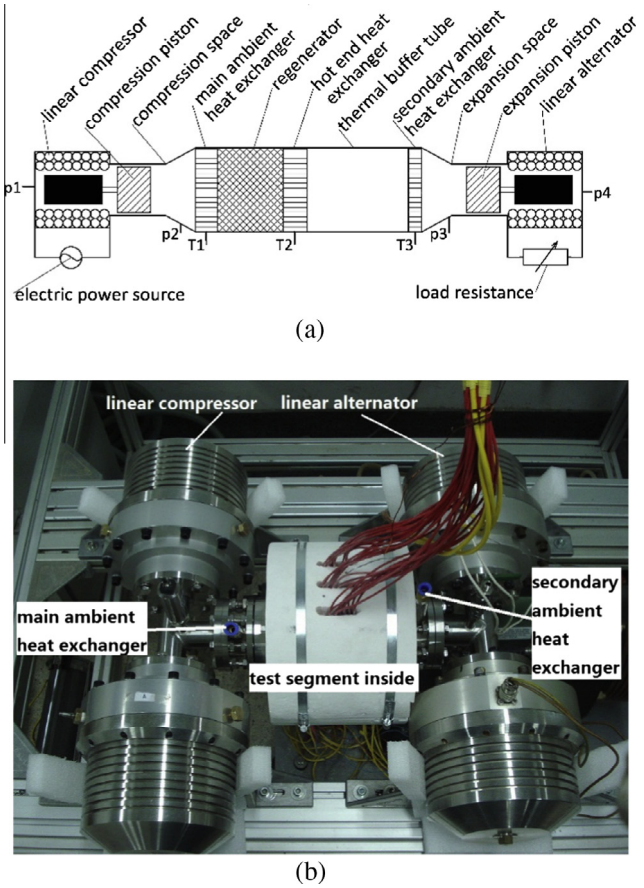

Fig. 1. Experimental setup: (a) schematic, (b) photograph.

Fig. 1(b) presents the photograph of our experimental setup. Here, four homemade 500 W class linear motors were used in the system, two motors acted as compressors and others served as alternators. Both the compressors and alternators were of dual-opposed configurations to reduce system vibration. The parameters of compression and expansion motors are listed in Table 1. The back space of one compression motor and one expansion motor were 1.72 l and 2.05 l, respectively. The linear motors had displacement and winding current limitations of 6.5 mm and 4 A (RMS). The regenerator was made of porous media, such as mesh screen, stack or random fiber. Stainless steel material was used to reduce the axial heat conduction of the regenerator. Electric heat cartridges were used to simulate the heating power put into the hot-end heat exchanger and the heating power should be adjusted during experiments to control the temperature of the hot-end heat exchanger. The hot parts of the system were surrounded by thermal isolation materials to reduce the heat loss. The temperature of the ambient heat exchangers are maintained at 293 K by cooling water. Structural dimension details of the thermoacoustic engine are presented in Table 2. The compression space and expansion space were 217 cc and 202 cc, respectively. In the experiments, the pressure waves in the front and back space of linear motors represented as p_1 to p_4 were measured by high-precision dynamic pressure sensors from PCB Piezotronics. And the temperature of three heat exchangers represented as T_1 to T_3 were measured by K type thermocouples. The voltages and currents of the compressors and alternators were monitored by high-precision voltage and current probes (model P5200 and TCP312) from Tektronix.

3. Theory

According to the transfer matrix method, the output parameters of any engine component have the relationship with the input parameters as

$$\begin{bmatrix} p_{\text{out}} \\ U_{\text{out}} \end{bmatrix} = \text{TM}_x \begin{bmatrix} p_{in} \\ U_{in} \end{bmatrix} \tag{1}$$

where TM_x is a two-by-two complex transfer matrix determined by the operation parameters and the structure parameters of the component. If we connect all components of the engine, we can obtain the relationship between the input and output parameters as

$$\begin{bmatrix} p_3 \\ U_3 \end{bmatrix} = \text{TM}_{es}\text{TM}_{shx}\text{TM}_{tbt}\text{TM}_{hhx}\text{TM}_{reg}\text{TM}_{mhx}\text{TM}_{cs} \begin{bmatrix} p_2 \\ U_2 \end{bmatrix} \tag{2}$$

Table 1
Mechanical and electrical parameters of the motors.

Parameter	Compressor	Alternator
D (mm)	60	50
M (kg)	1.66	1.1
K (kN m^{-1})	180	167.5
R_m (N s m^{-1})	16	22
r (Ω)	3.72	3.5
τ (N A^{-1})	97.7	94.1

Table 2
Structural parameters of the thermoacoustic engine.

Components	D (mm)	l (mm)
Main ambient heat exchanger	50	40
Regenerator	50	60
Hot-end heat exchanger	50	50
Thermal buffer tube	50	80
Secondary ambient heat exchanger	50	40

where the subscripts *es, shx, tbt, hhx, reg, mhx* and *cs* represent the expansion space, secondary ambient heat exchanger, thermal buffer tube, hot end heat exchanger, regenerator, main ambient heat exchanger and compression space, respectively. p_2 and p_3 are the pressure amplitudes before the pistons of the compressors and the alternators. U_2 and U_3 represent the volume velocity amplitudes provided by the compression and expansion pistons. Eq. (2) can be abbreviated for convenience as

$$\begin{bmatrix} p_3 \\ U_3 \end{bmatrix} = \begin{bmatrix} \text{TM}_{11} & \text{TM}_{12} \\ \text{TM}_{21} & \text{TM}_{22} \end{bmatrix} \begin{bmatrix} p_2 \\ U_2 \end{bmatrix} \tag{3}$$

According to the control equations of the linear alternator in the frequency domain [19]

$$\frac{\tau}{A}U_3 - (R + r + i\omega L)I = 0 \tag{4}$$

$$\frac{(R_m + i(\omega M - K/\omega))}{A^2}U_3 + \frac{\tau}{A}I = p_3 \tag{5}$$

From Eqs. (4) and (5), we can obtain the acoustic impedance of the linear alternator by eliminating I.

$$\frac{p_3}{U_3} = Z = \frac{1}{A^2}\left[R_m + i\left(\omega m - \frac{k}{\omega}\right) + \frac{\tau^2}{R + r + i\omega L}\right] \tag{6}$$

Solve Eqs. (3) and (6), we have the relationships between U_2 and U_3, $p2$ and $p3$ as

$$U_2 = \frac{Z \cdot \text{TM}_{21} - \text{TM}_{11}}{\text{TM}_{12}\text{TM}_{21} - \text{TM}_{11}\text{TM}_{22}}U_3 \tag{7}$$

$$p_2 = \frac{\text{TM}_{12}/Z - \text{TM}_{22}}{\text{TM}_{12}\text{TM}_{21} - \text{TM}_{11}\text{TM}_{22}}p_3 \tag{8}$$

According to Eqs. (7) and (8), for a given thermoacoustic heat engine with certain operation conditions, the phase angle difference between volume velocities and pressure waves are only determined by Z, i.e. the acoustic impedance of the linear alternator. We found that the phase differences between the input and output parameters can be easily controlled by changing the load resistance R. Actually, the phase angle of the pressure wave changes slightly along the regenerator even the engine, so the acoustic field at the regenerator is dominated by the volume velocity phase differences at the two ends of the engine. Additionally, it is worth noting that the moving masses of both linear alternators and linear compressors are very important during operation. For the alternator, a proper moving mass should be chosen to obtain the required phase difference range. For the compressor, the moving mass should be carefully designed to approach the mechanical resonant state and reduce the current value of the winding.

The thermoacoustic conversion performance of the regenerator is evaluated by the net output acoustic power and the thermoacoustic efficiency. The net output acoustic power is defined as the difference between the acoustic power consumed by the alternators and the inputted acoustic work by the compressors. According to the thermoacoustic theory, the generated acoustic power by the regenerator can be roughly calculated as

$$\delta W = \frac{1}{2}|p_3||U_3|\cos\theta_3 - \frac{1}{2}|p_2||U_2|\cos\theta_2 \tag{9}$$

where θ_2 and θ_3 represent the phase angle between the pressure and volume velocity of the compressor and alternator pistons. Actually, the acoustic work generated by the regenerator equals to δW plus some minor losses caused by flow resistances in the heat exchangers, thermal buffer tube and other places in the system. However, minor losses are small and difficult to measure. So, we simply regard δW as the generated acoustic work by regenerator.

The volume velocity amplitudes of the compressor and alternator can be obtained according to the pressure amplitude of the back space of the motors.

$$U_2 = -\frac{i\omega V_{cb}}{\gamma P_0} p_1 \tag{10}$$

$$U_3 = \frac{i\omega V_{eb}}{\gamma P_0} p_4 \tag{11}$$

where V_{cb} and V_{eb} represent the back space of compressor and alternator respectively. P_0 is the mean pressure. The negative sign in Eq. (10) means that the volume velocity of the compressor is in anti-phase with the pressure wave in the back space of the compressor, while the volume velocity of the alternator is in phase with the pressure wave in its back space as described by Eq. (11). Then, the phase angle difference between the volume velocities is

$$\Delta\theta_U = U_3 - U_2 \tag{12}$$

The thermoacoustic efficiency of the regenerator can be defined as:

$$\eta = \frac{\delta W}{Q} \tag{13}$$

where Q is the heating power.

4. Experimental results and analysis

In the experiments, 4.0 MPa helium was used as the working gas and the operating frequency was fixed at 80 Hz by a power source of the compressors. During the experiment, the input electric power of the compressors and the heating power of the hot end heat exchanger should be adjusted to fix a displacement of the alternators of 6 mm as well as a heating temperature of 650 °C. In order to avoid the alternator being damaged by large coil current, the load resistance should be larger than 30 Ω to control the current within 4 A (RMS).

4.1. Influence of phase difference

In the regenerative heat engines, the acoustic field constructed by the phase difference between the pressure wave and volume velocity oscillation in the regenerator plays a crucial role in the thermoacoustic conversion process. Because the pressure phase angle changes very small across the regenerator even the engine, the acoustic field of the regenerator is mainly dominated by the velocity phase angles at its two ends. However, the velocity phase angles information in the regenerator was very difficult to be measured, so the phase angle difference between the movements of the compression and expansion pistons was used to evaluate the regenerator performance in this paper.

Fig. 2 shows the volume velocity phase difference $\Delta\theta_U$ between the compression and expansion pistons as a function of the load resistance of the alternator with different heating temperatures. In the experiments, the regenerator was made of many pieces of 150 mesh stainless steel screen with wire diameter of 60 μm and porosity of 73.6%. In Fig. 2, it can be seen that $\Delta\theta_U$ increases from about −152° to −125° because of the impedance variation of the expansion motor by changing the load resistance. Moreover, the phase angle seems almost independent on the heating temperature, which means very slight influence of the heating temperature on the transfer matrices of all engine components. Fig. 2 verifies that the phase difference between the volume velocities at two ends of the engine could be greatly changed by changing load resistance of the alternator. However, due to the current limitation of the alternator, the phase difference could not be improved any more.

Fig. 3 presents the load resistance dependences of the net output acoustic power and thermoacoustic efficiency with different heating temperatures. According to Fig. 3, the net output acoustic power increased with the decrease of load resistance due to the increase of the input acoustic power presented in Fig. 4. That is, when the phase angle approached −120°, more acoustic power

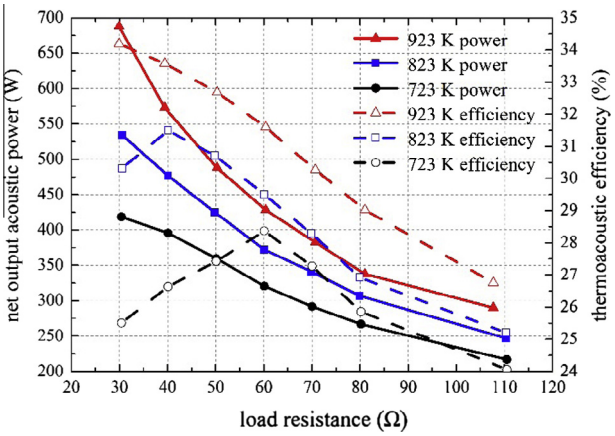

Fig. 3. Net output acoustic power and thermoacoustic efficiency vs. load resistance with different heating temperatures.

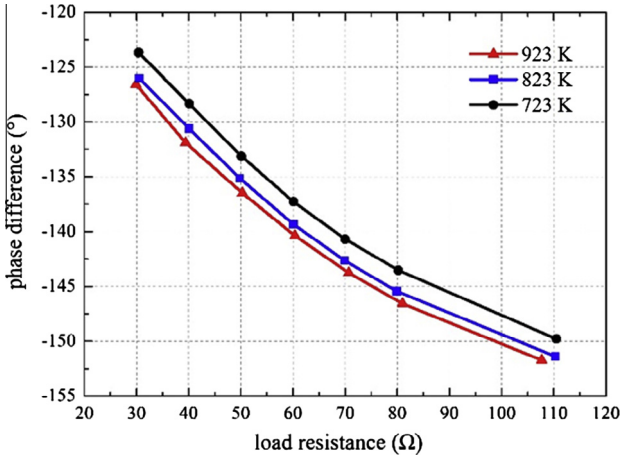

Fig. 2. Phase difference between compression and expansion pistons vs. load resistance with different heating temperatures.

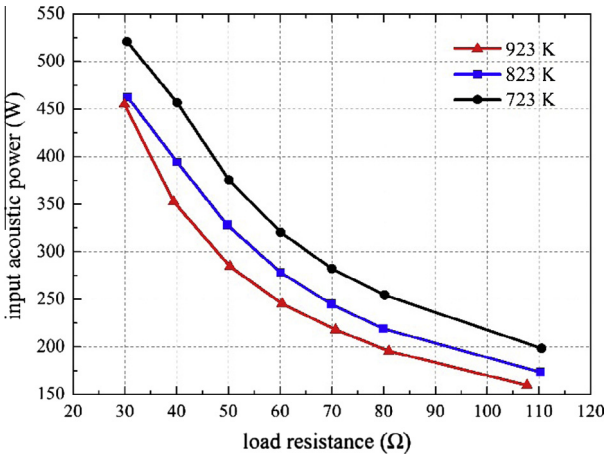

Fig. 4. Input acoustic power of the compressor vs. load resistance with different heating temperature.

could be inputted to the regenerator and more net acoustic power could be produced by the regenerator while the volume velocity of the alternator was fixed during the experiments. However, because of the current limitation of the motor winding, the maximum output acoustic powers were 688 W, 570 W and 419 W with the heating temperatures of 923 K, 823 K and 723 K, respectively. Additionally, the thermoacoustic efficiency had an optimum value for 823 K and 723 K heating temperature, while the optimum value was not obtained for 923 K heating temperature because of the current limitation. It could be also found that the maximum thermoacoustic efficiency increased as the heating temperature raised. It could be easy to imagine that the maximum thermoacoustic efficiency of 923 K heating temperature would be much higher than that of 723 K. It also indicated that the regenerator should be designed to work in an optimum acoustic field to achieve a high efficiency with a certain heating temperature. However, in a real engine, one should balance between a high acoustic power production to improve the system power density and a high efficiency.

4.2. Influence of regenerator type

Generally, regenerator is a porous medium with very irregular and complicate flow channels for the working gas. The design of the regenerator is always a compromise between the good thermoacoustic conversion capacity and the low flow resistance. However, the regenerator performance is strongly dependent with the technology arts of fabrication and is very difficult to be precisely predicted by numerical method, thereby needs experimental measurement. In this experiment, three different types of regenerators were studied, which were widely used in the regenerative heat engines. First one was made of 150 mesh stainless steel screen with wire diameter of 60 μm, hydraulic radius of 41.8 μm and porosity of 73.6%. Second one was the stack made of stainless steel pieces with uniform flow channels produced by chemical etching with a gap of 120 μm, hydraulic radius of 60 μm and porosity of 66.7%. The last one was sintered random fiber made of 30 μm stainless steel silk with hydraulic radium of 39.4 μm and porosity of 84%. The hydraulic radius of the regenerator is calculated by

$$r_h = d_{wire}\frac{\phi}{4(1-\phi)} \tag{14}$$

Sample pieces of three type of regenerator materials were demonstrated in Fig. 5. The regenerators was made of many sample pieces with the same diameter and the length. The heating temperature was fixed at 923 K and the other experimental conditions were as same as those in Section 4.1. The thermal penetration depth of helium and stainless steel at cooling, heating and average temperatures are presented in Table 3 according to Eq. (15). Usually, the thermal penetration of helium is much larger than the hydraulic radius of the regenerator to have a good heat exchange between the solid and gas. The thermal penetration depths of the gas and solid are always used as a rough guidance in choosing parameters of regenerator material.

Table 3
Thermal penetration depth of helium and stainless steel.

	293 K	923 K	611.5 K
δ_{k_he} (mm)	0.132	0.354	0.249
δ_{k_ss} (mm)	0.126	0.136	0.132

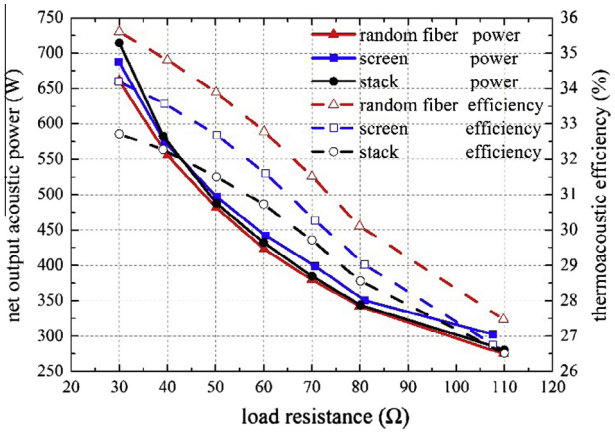

Fig. 6. Net output acoustic power and thermoacoustic efficiency vs. load resistance with different regenerator types.

$$\delta_k = \sqrt{\frac{2k}{\omega\rho C_p}} \tag{15}$$

Fig. 6 presents the curves of net output acoustic power and thermoacoustic efficiency as functions of load resistance with different regenerator types. From Fig. 6, it could be seen that a maximum net output acoustic power of 715 W was obtained with stack type regenerator and a maximum thermoacoustic efficiency of 35.6% W was achieved with random fiber type regenerator. Since the phase angles of three types of regenerators were almost the same shown in Fig. 7, the difference between the net output acoustic powers with three regenerator types was mainly determined by flow resistance loss. Fig. 8 gives the amplitudes of the pressure waves in the compression and expansion spaces with different load resistances. Because the displacement of the alternators were fixed at 6 mm, the pressure amplitudes in the expansion space represented by dashed line in Fig. 8 were quite similar. So, the amplitudes of the pressure waves in the compression spaces could reflect flow resistance of the regenerators. From Fig. 8, it could be seen that the pressure wave amplitude of the stack in the compression space was much smaller than screen and random fiber, which meant a smaller flow resistance loss of the stack

Fig. 5. Different types of regenerator pieces. (a) Stack (b) mesh screen (c) random fiber.

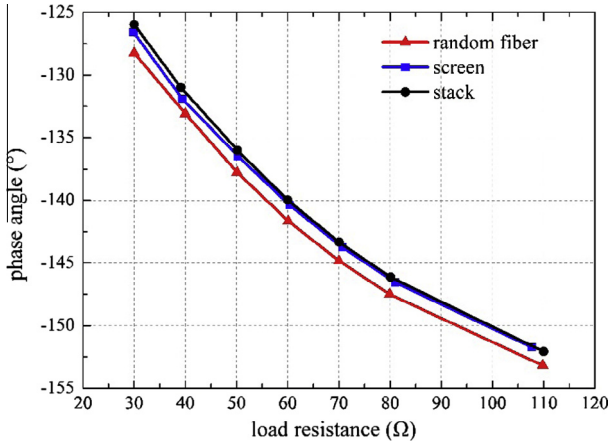

Fig. 7. Phase angle vs. load resistance with different regenerator types.

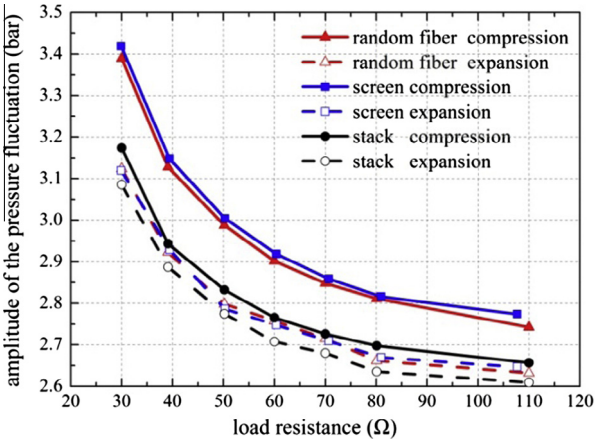

Fig. 8. Pressure amplitudes vs. load resistance with different regenerator types.

regenerator. As a result, the stack type regenerator could produce more acoustic work. However, the random fiber regenerator had the larger thermoacoustic efficiency than the stack. The reason was possibly due to the different heat transfer area between gas and solid in the regenerator. Large heat transfer area meant sufficient heat exchange and small heat transfer loss. The heat transfer area of the screen and random fiber could be calculated by

$$A_h = \frac{4V(1-\phi)}{d_{wire}} \tag{16}$$

And the heat transfer area of the stack could be calculated by

$$A_h = \frac{2V\phi}{d_{gap}} \tag{17}$$

where V was the volume of the regenerator. According to Eqs. (16) and (17), the random fiber regenerator had a transfer area of about 2.5 m^2, which was much higher than that of 1.3 m^2 of the stack regenerator. According to these results, a perfect regenerator possibly has regular flow channel to reduce the flow resistance and has sufficient contact area between working gas and solid wall to reduce heat transfer loss.

5. Conclusions

In this paper, a novel test platform was developed to investigate the thermoacoustic conversion characteristic of the regenerator. Linear compressors and alternators were used to obtain a required phase angle by changing the load resistance of the alternator. In our experiments, the influence of phase angle with different heating temperatures and different types of regenerator materials on the performance were studied in detail. The experimental results indicated that the net output acoustic power and the maximum thermoacoustic efficiency increased as the increase of the heating temperature. The velocity phase difference between the two ends of the engine was critical to the performance of regenerator, the net output acoustic power increased as the phase angle closed to 120° while the thermoacoustic efficiency had an optimum value. In the experiments, a maximum output acoustic power of 715 W and a highest thermoacoustic efficiency of 35.6% were obtained with stack type and random fiber type regenerators respectively under 4 MPa pressurized helium and 650 °C heating temperature. The performance of different types of regenerators show that the balance between the low flow resistance and high heat transfer area was crucial to design a regenerator for the regenerative heat engines. This work provided an efficient way to investigate the thermoacoustic conversion characteristic of the regenerator. Additionally, it was believed that this work could provide useful clues to improve the performance of the regenerator.

Acknoeledgements

This work is financially supported by National Natural Science Foundation of China (51276186) and Beijing Natural Science Foundation (3132034).

References

[1] Ceperley PH. A pistonless Stirling engine-the traveling wave heat engine. J Acoust Soc Am 1979;66(5):1508–13.
[2] Rott N. Damped and thermally driven acoustic oscillations in wide and narrow tubes. ZAMP 1969;20(2):230–43.
[3] Rott N. Thermally driven acoustic oscillation. Part II: Stability limit for helium. ZAMP 1973;24(1):54–72.
[4] Rott N. Thermally driven acoustic oscillation. Part III: Second-order heat flux. ZAMP 1975;26(1):43–9.
[5] Swift GW. Thermoacoustic engines. J Acoust Soc Am 1988;84(4):1145–80.
[6] Backhaus S, Swift GW. A thermoacoustic-Stirling heat engine: detailed study. J Acoust Soc Am 2000;107(6):3148–66.
[7] Xiao JH. Thermoacoustic heat transportation and energy transformation Part 1: Formulation of the problem. Cryogenics 1995;35(1):15–9.
[8] Xiao JH. Thermoacoustic heat transportation and energy transformation Part 2: Isothermal wall thermoacoustic effects. Cryogenics 1995;35(1):21–6.
[9] Xiao JH. Thermoacoustic heat transportation and energy transformation Part 3: Adiabatic wall thermoacoustic effects. Cryogenics 1995;35(1):27–9.
[10] Ueda Y, Biwa T, Mizutani U, et al. Acoustic field in a thermoacoustic Stirling engine having a looped tube and resonator. Appl Phys Lett 2002;81(27):5252–4.
[11] Biwa T, Tashiro Y, Mizutani U. Experimental demonstration of thermoacoustic energy conversion in a resonator. Phys Rev E 2004;69(6):066304.
[12] Lawn C. Acoustic pressure losses in woven screen regenerators. Appl Acoust 2014;77:42–8.
[13] Kato Y, Baba K. Empirical estimation of regenerator efficiency for a low temperature differential Stirling engine. Renew Energy 2014;62:285–92.
[14] Guoyao Yu, Luo Ercang, Dai Wei, Jianying Hu. Study on several important nonlinear processes of a large experimental thermoacoustic-Stirling heat engine using computational fluid dynamics. J Appl Phys 2007;102:74901–7.
[15] Rulik S, Remiorz L, Dykas S. Application of CFD technique for modelling of the thermoacoustic engine. Arch Thermodyn 2011;32(3):175–90.
[16] Nowak Iwona, Rulik Sebastian, Wróblewski Włodzimierz, Nowak Grzegorz, Szwedowicz Jarosław. Analytical and numerical approach in the simple modelling of thermoacoustic engines. Int J Heat Mass Transf 2014;77:369–76.
[17] Yadava CO, Joshib UV, Patel LN. CFD assisted prediction of hydrodynamic parameters for regenerator of cryocooler. Proc Technol 2014;14:328–35.
[18] Rout SK, Gupta AK, Choudhury BK, Sahoo RK, Sarangi SK. Influence of porosity on the performance of a pulse tube refrigerator: a CFD study. Proc Eng 2013;51:609–16.
[19] Swift GW. Thermoacoustics: a unifying perspective for some engines and refrigerators. Sewickley: Acoustical Society of America Publications; 2002.